ELSEVIER

Computers in Biology and Medicine 38 (2008) 555–562

Computers in Biology and Medicine

www.intl.elsevierhealth.com/journals/cobm

Finite element analysis of blood flow and heat transfer in an image-based human finger

Ying He[a,c,*], Hao Liu[b], Ryutaro Himeno[a], Junko Sunaga[a], Nobunori Kakusho[a], Hideo Yokota[a]

[a] *Computational Biomechanics Unit, RIKEN, 2-1 Hirosawa, Wako-shi, Saitama 351-0198, Japan*
[b] *Faculty of Engineering, Chiba University, 1-33 Yayoi-cho, Inage-ku, Chiba 263-8522, Japan*
[c] *Department of Modern Mechanics, University of Science and Technology of China, Mail Box 4, Hefei, Anhui 230027, PR China*

Received 18 May 2006; accepted 1 February 2008

Abstract

The human finger is said to be the extension of the brain and can convey the information on mechanical, thermal, and tissue damaging. The quantitative prediction of blood flow rate and heat generation are of great importance for diagnosing blood circulation illness and for the noninvasive measurement of blood glucose. In this study, we developed a coupled thermofluid model to simulate blood flow in large vessels and living tissue. The finite element (FE) model to analyze the blood perfusion and heat transport in the human finger was developed based on the transport theory in porous media. With regard to the blood flow in the large arteries and veins, the systemic blood circulation in the upper limb was modeled based on the one-dimensional flow in an elastic tube. The blood pressure and velocity in each vessel were first computed and the corresponding values for the large vessels in the finger were subsequently transferred to the FE model as the boundary conditions. The realistic geometric model for the human finger was constructed based on the MRI image data. After computing the capillary pressure and blood velocity in the tissue, the temperatures in the large vessels and the tissue of the finger were computed simultaneously by numerically solving the energy equation in porous media. The computed blood flow in tissues is in agreement with the anatomical structure and the measurement. It is believed that this analysis model will have extensive applications in the prediction of peripheral blood flow, temperature variation, and mass transport.

Keywords: Porous media; Blood perfusion; Finite element method; One-dimensional blood flow; Human finger; Image-based model; MR images

1. Introduction

Blood circulation performs an important function—to carry oxygen to the tissues and to remove carbon dioxide and other metabolites from the tissues. Thus, blood circulation plays a crucial role in thermoregulation and mass transport. The quantitative prediction of the relationship between hemodynamics and heat and mass transfer is of great interest, because it is related to human thermal comfort, drug delivery, and noninvasive measurement. For example, Cho et. al. [1] proposed a noninvasive method for measuring glucose, where glucose is derived by measuring heat generation, blood flow rate, and hemoglobin oxygenation in a person's fingertip.

Biological tissues contain blood and the surrounding materials where blood is perfused to tissues via capillary network. The energy transport in tissues includes conduction in tissues, convection between blood and tissues, perfusion through microvascular beds, and metabolic heat generation. Among these, the heat transfer between blood and tissues could be of the greatest importance. The use of Pennes [2] bioheat equation is the most common method available to describe blood perfusion in the tissue. However, this method cannot explain the convection between large vessels and tissues but only explain the uniform perfusion of blood to tissues.

Further, in another method, the spatial variations in the arterial, venous, and tissue temperatures are considered, and it includes three equations that represent the heat transfer in arteries, veins, and tissues. This method was first presented by Keller and Seiler [3] and has been developed and used by many other researchers [4–8]. These models are frequently applied in describing the whole body thermal system.

* Corresponding author at: Department of Modern Mechanics, University of Science and Technology of China, Mail Box 4, Hefei, Anhui 230027, PR China. Tel./fax: +86 551 3602477.
E-mail address: yhe@ustc.edu.cn (Y. He).

0010-4825/$ - see front matter © 2008 Elsevier Ltd. All rights reserved.
doi:10.1016/j.compbiomed.2008.02.002

Researchers also intend to analyze heat transfer in living tissues by modeling the detailed countercurrent microvascular network. Chen and Homes [9] presented a bioheat transfer model that accounts for the thermally significant blood vessels. They treated the blood vessels as two groups—large vessels and small vessels. Each vessel is treated separately in the former group, whereas all vessels are treated as a part of a continuum in the latter group. The thermal contributions of the small blood vessels were considered from the equilibration of blood temperature, convection of the flowing blood, and the small temperature fluctuations of the nearly equilibrated blood. Weinbaum and Jiji [10] proposed an alternative model that accounts for the thermal effect of the directionality of the blood vessels and the characteristic geometry of the blood vessel arrangement. The vascular structure in the periphery was treated individually rather than as continuum media in their three-layer model. Brinck and Werner [11] presented a three-dimensional thermal and vascular model in which the convective heat exchange between the feeder vessels and tissue was computed by the values for the Nusselt number, and the temperatures in and near individual vessels were predicted. The thermally significant vessels were treated individually according to their distribution characteristics in different tissue layers.

From these modeling studies, it is evident that investigation of the thermal effects of large blood vessels and small vessels is the most important aspect. However, due to the high density and complex arrangement of microvessels, little information about vascular geometry can be obtained and the applications of the vascular models are limited for small volumes of tissue. Thus, it is of great importance to develop an easy-to-use model for describing the blood flow in different sizes of vessels.

On the other hand, a blood-perfused biological tissue can be described as a porous medium in which the fluid phase represents the blood and the surrounding tissue is represented by the solid phase. The theory of porous media for heat transfer in living tissues may be the most appropriate since it can describe the perfused blood with fewer assumptions as compared to other bioheat model [12]. Wulff [13] first dealt with the living tissue as a porous medium and utilized the convective term, including the Darcy velocity, to replace the blood perfusion term in the bioheat equation. Xuan and Roetzel [14] used the transport theory through porous media to model the tissue–blood system. The blood and tissue were considered to be in a non-equilibrium state and two energy equations were used to express heat transfer in the blood phase and solid phase. The advantage of this model is that it includes the exact blood perfusion in tissues, blood dispersion, and effective tissue conductivity and is considered to be appropriate for modeling a blood-perfused tissue. However, the flow in large blood vessels differs from the filtration flow through tissues and may be considered separately.

Mesh generation based on the realistic geometric model is also of significance in performing thermal analysis in the living tissue. Geometrical modeling and mesh generation based on medical images (CT or MR images) are widely used in biofluid mechanics and biomechanics analysis [15,16]. The conventional steps to construct a computational model are image processing, geometrical modeling, and mesh generation. Although the techniques in medical imaging and geometrical modeling need to be integrated, the image-based modeling technique provides a rapid and valid method to model the thermofluid and mechanics problems in living tissues.

The purpose of this study is to model blood–tissue heat transfer according to the different characteristics of blood flow in large vessels and tissues. The systemic blood circulation in the upper limb has been modeled based on the one-dimensional flow in an elastic tube, and the finite element (FE) model based on the heat transport in porous media was developed to analyze the blood perfusion and heat transport in the human finger. Further, the realistic geometric model for the human finger was constructed on the basis of MR image data. After computing the capillary pressure and blood velocity in the tissue, the temperatures of the large vessels and the finger tissue were computed simultaneously by numerically solving the energy equation in the porous media.

2. Modeling blood flow dynamics and heat transfer in tissues

The basic insight in modeling blood flow is that the use of different models to simulate blood flow in large vessels (The diameter is larger than or equal to 1 mm) and in microvessels. A non-linear one-dimensional flow model in an elastic tube is used to express blood flow in large vessels, whereas blood flow perfused in tissues is considered as the fluid phase in the porous media. The unified energy equation is used to model the heat transfer in large vessels and tissues.

2.1. Blood flow dynamics

The blood flow in large vessels has been modeled to be a one-dimensional flow in an elastic tube, and the governing equations, including continuity and momentum, are expressed as

$$\frac{\partial A}{\partial t} + \frac{\partial q}{\partial x} = 0, \tag{1}$$

$$\frac{\partial q}{\partial t} + \frac{\partial}{\partial x}\left(\frac{q^2}{A}\right) + \frac{A}{\rho}\frac{\partial P}{\partial x} = -\frac{2\pi v r}{\delta}\frac{q}{A}, \tag{2}$$

where x is the distance from the heart, t is the time, A is the cross-sectional area of the blood vessel, q is the blood flow rate, P is the transmural pressure, ρ is the blood density, v is the kinematic viscosity, δ is the boundary-layer thickness, and r is the radius of the blood vessel.

The pressure–area relationship for the arteries and veins is as follows:

$$P(x,t) - P_0 = \frac{4}{3}\frac{Eh}{r_0}\left(1 - \sqrt{\frac{A_0}{A}}\right), \tag{3}$$

$$p - p_0 = k_p\left[1 - \left(\frac{A}{A_0}\right)^{-3/2}\right], \tag{4}$$

where E is Young's modulus, h is the wall thickness of the blood vessel, and k_p is the coefficient that is proportional to the bending stiffness of the tube wall.

A periodic flow wave was assigned at the inlet boundary, and a constant pressure was assigned at the outlet. With regard to the bifurcation conditions and the junction conditions between two equivalent tubes, it is assumed that there is no leakage of blood at the bifurcations, the inflow and outflow are balanced, and the pressure is continuous.

The two-step Lax–Wendroff method has been widely used in analyzing blood flow of one-dimensional model [17–19]. In order to compute the blood flow rate and the variation of cross-sectional area, He et al. [20] employed the same scheme as that in Zagzoule et al. [19]. The detailed numerical method can be found in the literature [20].

2.2. Darcy model and energy equation for biological tissues

The Darcy model is considered to be the earliest flow transport model in porous media and is expressed as

$$\nabla P = -\frac{\mu}{K}\mathbf{v}, \tag{5}$$

where K is the permeability of the tissues, μ is the viscosity, and $\mathbf{v}$ is the Darcy velocity.

Considering the continuity equation and momentum equation, the dimensionless pressure in porous media is expressed as

$$\frac{\partial^2 P^*}{\partial x^{*2}} + \frac{\partial^2 P^*}{\partial y^{*2}} = 0. \tag{6}$$

The dimensionless velocity is expressed as

$$u^* = -Da\,\mathrm{Re}\,\frac{\partial P^*}{\partial x^*}, \tag{7}$$

$$v^* = -Da\,\mathrm{Re}\,\frac{\partial P^*}{\partial y^*}, \tag{8}$$

where Da is the Darcy number and is expressed as

$$Da = \frac{K}{D^2}. \tag{9}$$

According to the energy equation for the local equilibrium state between solid tissues and blood flow [23], the dimensionless energy equation can be expressed as follows:

$$\frac{\partial T^*}{\partial t^*} + \varepsilon\left[u^*\frac{\partial T^*}{\partial x^*} + v^*\frac{\partial T^*}{\partial y^*}\right] = \frac{1}{Pe_m}\left[\frac{\partial^2 T^*}{\partial x^{*2}} + \frac{\partial^2 T^*}{\partial y^{*2}}\right] + \frac{1}{Pe_m}q_m^*, \tag{10}$$

where Pe_m, ε, and q_m^* are expressed as follows:

$$Pe_m = \frac{U_\infty D}{\alpha_m}, \tag{11}$$

$$\varepsilon = \frac{(\rho c)_b}{(\rho c)_m}, \tag{12}$$

$$q_m^* = \frac{q_m D^2}{(T_a - T_\infty)k_m}. \tag{13}$$

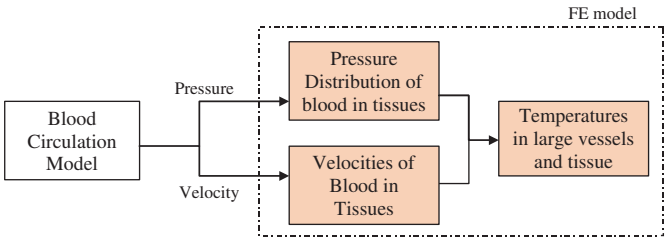

Fig. 1. Flow chart of the computational method.

Eq. (10) can be suitably applied for heat transport in both large vessels and tissues. When it is applied to the heat transport in large vessels, both ε and φ attain a value of 1.

Eqs. (6)–(8) and (10) have been discretized using the finite element method (FEM), and the finite element equation has been developed using the Galerkin weighted residual method. First, the conjugate gradient (CG) method was employed to solve Eq. (6). The value of the pressure in the large vessels was obtained from the blood flow model and was assigned as the boundary condition of Eq. (6). Second, the blood flow velocities in the tissues were computed. The slip condition was employed at the large vessel wall. Finally, the temperatures in large vessels and tissues were computed simultaneously. A constant blood temperature condition was assigned to an inlet of a large artery in the finger. The heat transfer at the skin surface is due to heat convection, radiation, and evaporation. The flowchart of the computational method is shown in Fig. 1.

3. Geometrical modeling for the human finger from MR images

Since we use a one-dimensional flow model to describe the blood flow in arteries and veins, the data for the initial cross-sectional area and the length of the blood vessel are required. The dimensions of larger vessels are from the data in literature [17] and [18] where the data are obtained by anatomical measurements. Since there are few available data for the dimensions of smaller vessels, the data for this part in our model are from the deduced data by Sheng et al. [17].

3.1. MR image acquisition

The original images were acquired for a volunteer's finger. A hand-fitted supporter made of silicon rubber was produced in order to fix the volunteer's hand before taking images. A 1.5-T scanner (Excelart, Toshiba Medical Systems) was used with different sequence for taking the images of blood flow and different tissues. The image resolution is 128 × 128 and 256 × 256, respectively, and the slice thickness was set to be 1.5 mm. A circular coil whose diameter fitted the length of the volunteer's finger was employed. Fig. 2a and b are the original MR images of the finger in the vertical and lateral directions, and Fig. 2c is the MR image of the blood flow in the finger.

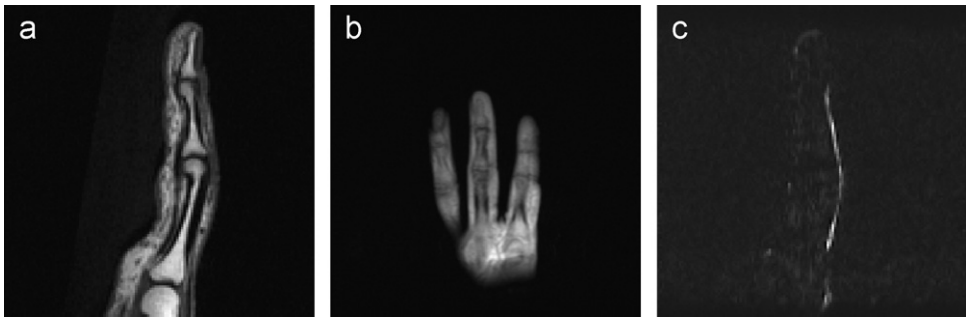

Fig. 2. (a) Original MR image of the human finger in the vertical direction; (b) original MR image of the human finger in the lateral direction; and (c) original MR image of the blood flow in the human finger.

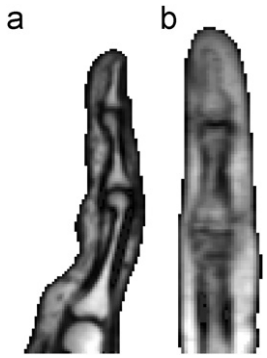

Fig. 3. The images of the human finger after image processing: (a) in the vertical direction and (b) in the lateral direction.

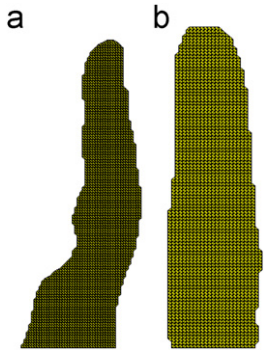

Fig. 4. The FE models constructed from processed images: (a) vertical direction and (b) lateral direction.

Table 1
The text file of the MR image

0	0	0	0	0	0	0	16	26
0	0	0	0	0	4	23	40	54
0	0	0	0	5	24	46	59	67
0	0	0	4	21	43	63	72	68
0	0	2	17	33	57	69	72	62

3.2. Edge detection

In order to obtain the boundary of the finger, the original images were firstly processed by enhancing contrast and arithmetic subtracting through an image analysis program Scion Image [21]. Hence, an image only with the information of the objected finger was acquired. Fig. 3a and b show the processed results. Scion Image [21] has the function to export the image as a text file, thus, the processed image can be exported as a text file where the brightness of each pixel in the image is expressed in a matrix by color indices from 0 to 255. Table 1 shows one part of the text file of the image in which the numbers represent the brightness of every pixel. The area where the brightness number is 0 represents the area outside the finger and the area where the brightness number is not zero represents the finger. The finger area can be known by identifying the pixels whose color indices are not zero.

3.3. Mesh generation

The text file for the image was thus input into the original mesh generation program and the nodes for the finger can be counted directly from the text file. This process is written in the program as follow:

```
c- - - - -Read the pixel data- - - - - - - - - - - - - - - - - - - - -
c- - - - -the size may be 128 or 256
 do j = 1, 128
  read(100,*) (color(i, j), i = 1, 128)
 end do
 ……
c- - - - - - -count the node number- - - - - - - - - - - -
 if(color(i, j).ne.0) then
  nodenum = nodenum + 1
  nx(nodenum) = x(i, j)
  ny(nodenum) = y(i, j)
```

The adjacent four nodes in x and y direction formed a square element which can be divided into two adjacent triangular elements. Fig. 4a and b show the original FE models when the node distance in x and y directions is set to be one pixel in mesh generation.

For the thermofluid computation, the surface of the finger in the original model requires smoothing. The smoothing approach is to fit discrete surface areas by linear interpolation and generate meshes over these areas. First, the discrete points

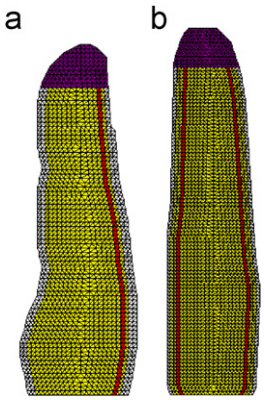

Fig. 5. The finite element model for the computation with different materials: (a) in the vertical direction and (b) in the lateral direction.

in the surface were identified and the straight lines were connected between two adjacent discrete points. Second, interior nodes were generated within the two points and new triangular elements were created over this discrete area. Finally, the node distance in x direction was regulated such that the meshes around the boundary part were fine and those in the interior part were coarse in x direction. Note that the regulation of mesh size was carried out only in x direction, whereas the node distance in y direction still remained the same as one pixel.

3.4. Material identification

As shown in Fig. 2c, the large artery in the human finger can be detected. Regarding the blood vessels with a diameter smaller than that of the large artery, we assumed that they were the fluid phase in the porous media. The position of the represented pixel expressing large artery was identified and the coordinate information was added to the FE model. Thus, the arterial vessel part was classified from the other parts. The nodes neighbored to the arterial nodes were set to be the vein and the fingertip part was identified according to the characteristic points in the original MR image. Thus, the FE models for the computation were constructed as shown in Fig. 5a and b in which different materials have been expressed in different colors.

4. Computation results

The thermophysical properties have been listed in Table 2, which are referred to the references [7,22]. It is considered that the porosity of the tissue does not normally exceed 0.6 [23]. Based on the data in [22], we defined the porosity in the bone, tendon, skin, and fingertip as 0, 0.1, 0.2, 0.3, respectively. Due to the large density of the vessels in the fingertip, the porosity was assigned a larger value. Tissue permeability was defined as $10^{-13}\,m^2$ [23]. Fig. 6 shows the variation of pressure in the large arteries and veins in the finger which is computed by the one-dimensional blood flow model. It can be observed that the pressure difference is greater in the artery, whereas there is only a slight difference in the vein. These data were assigned

Table 2
Physical properties and porosities

	Bone	Tendon	Skin	Fingertip	Blood
ρ (kg/m^3)	1418	1270	1200	1270	1100
c (J/kg K)	2094	3768	3391	3768	3300
λ (W/mK)	2.21	0.35	0.37	0.35	0.50
q_{meta} (W/m^3)	170	632	250	632	
φ	0.0	0.1	0.2	0.3	1.0

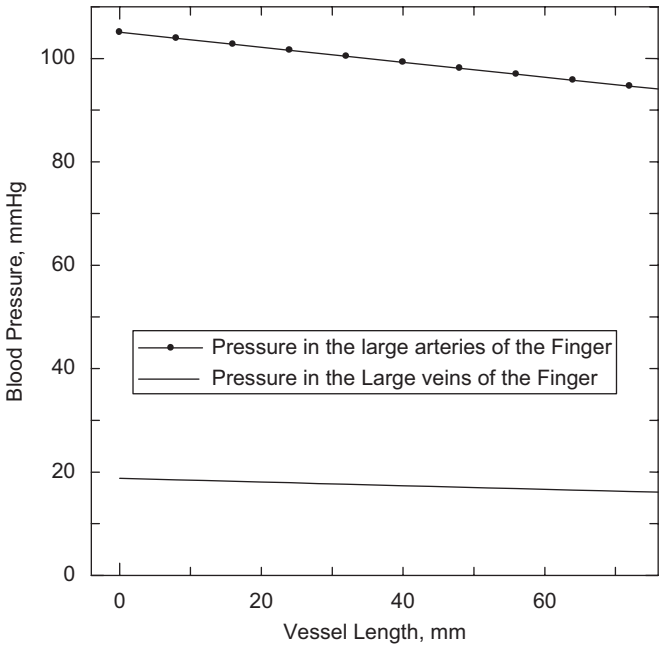

Fig. 6. Pressure distribution in the axial direction of the blood flow in large arteries and veins of the finger.

to the nodes that represent the artery and vein in the FE model and the pressure was set such that it varied along the blood flow direction but did not change in the direction normal to the flow direction.

The inflow velocities in the finger artery and vein are 19 cm/s and 3.5 cm/s, respectively, according to the computation results from one-dimensional model, and the Reynolds number in the computation is 50 when the arterial velocity is the reference velocity. Since the computed velocity along the flow direction slightly changes in the large vessels, it is assigned to the blood nodes with uniform values.

Figs. 7(a) and (b) show the computed capillary pressure and flow distribution of the finger model in the vertical direction. It can be observed that the pressure difference is obvious in the fingertip and the blood flow (Fig. 7(b)) is greater than that in other areas. Fig. 7(c) shows the temperature distribution in the large vessels and tissues in the vertical section of the finger when the environmental air temperature is 22 °C. It can be observed that the blood temperature in the arteries is relatively higher. The temperature difference between arterial and tissue temperature can be observed more clearly in Fig. 8 where the temperature profile in different position is plotted. It can be seen

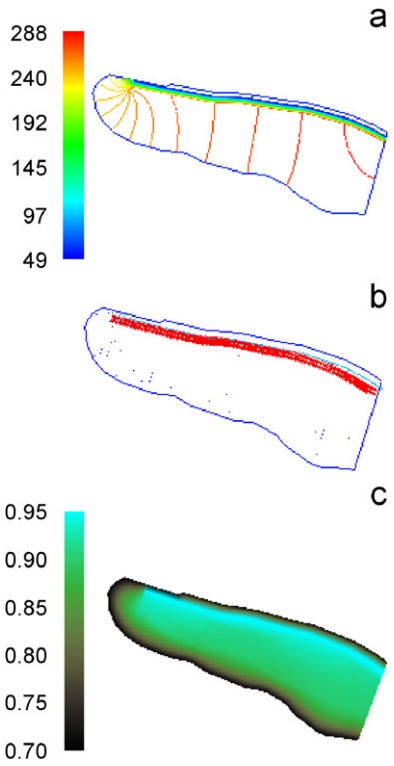

Fig. 7. (a) The computed capillary pressure, (b) velocity, and (c) temperature in the image-based model of the human finger.

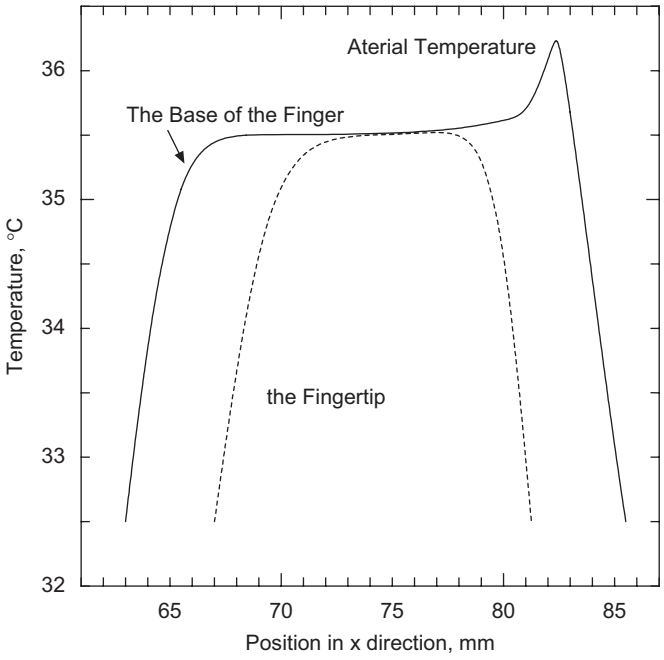

Fig. 8. Temperature profiles in the fingertip and base of the human finger for vertical section model.

that the arterial blood temperature is markedly higher, whereas the temperature of the venous blood has not distinguished difference than that of the surrounding tissue; this implies that the

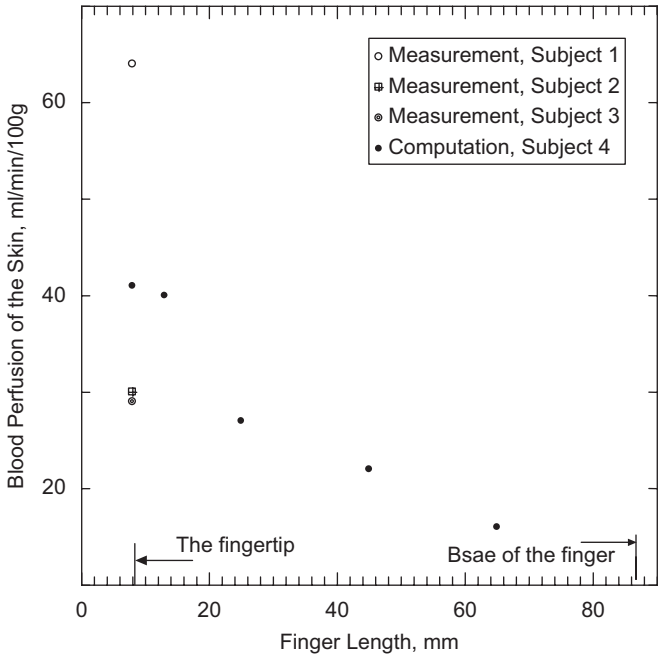

Fig. 9. Blood perfusion of the skin in different position of the human finger.

effect of convection in the venous vessel is not as large as that in the arterial vessel.

If we assume that the diameter and the length of the microvessels are the same in different place of the tissue, the rate between the microvessel blood flow and microvessel volume can be written as

$$\frac{Q_b}{V_b} = \frac{v}{l}, \tag{14}$$

where v is the blood velocity and l is the length of microvessel. Since the microvascular volume is written as $V_b = \varphi V_t$, the blood perfusion can be expressed as

$$\text{perfusion} = \frac{Q_b}{V_t} = \frac{v_{Darcy}}{l}. \tag{15}$$

Hence, the blood perfusion can be obtained from the Darcy velocity according to Eq. (15). Fig. 9 shows the blood perfusion of the skin in different position of the human finger. It can be seen that the blood perfusion from the fingertip to the base gradually decreases, which is in agreement with the anatomical structure of the finger. The measurements of the blood perfusion of the skin in the fingertip are also plotted in Fig. 9. We can see that although the measured value changes considerably due to different subjects, the computational value is in the reasonable range.

The computed results using another image-based model in the lateral direction are shown in Fig. 10(a)–(d). As similar in Fig. 7(a) and (b), an obvious pressure difference existed in the fingertip, thus the blood flow in the fingertip is larger. The anatomical structure of the finger [24] is shown in Fig. 10 (c), where the larger density vessels can be observed. The temperature distribution in large vessels and tissues is

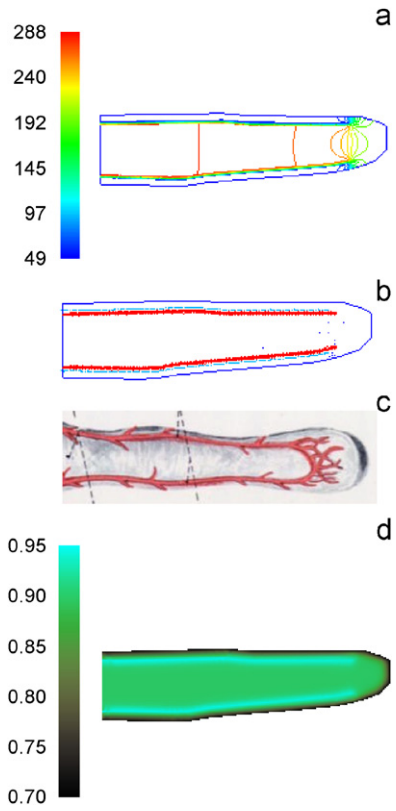

Fig. 10. (a) The computed capillary pressure, (b) velocity, (c) the anatomical structure of the blood vessels in the finger [24], and (d) temperature distribution in the human finger model of the lateral direction.

shown in Fig. 10(d), where the temperature in the fingertip remains smooth variation due to the larger blood perfusion in this part.

5. Discussion and conclusions

In this study, we divided the blood flow in the tissues into two groups: one is the blood flow in the large vessels (the diameter of the vessels is generally larger than or equal to 1 mm) and the other is the blood flow in the microvessels. We used a one-dimensional flow model in an elastic tube to describe the blood flow in the large vessels, and the Darcy model to model the flow in porous media to describe the blood flow in microvessels. The unified energy equation was used to model the heat transfer in larger vessels and in the tissue that was considered as porous media. The computed results have shown that the simulated blood flow through tissues is qualitatively in agreement with the anatomical structure and the measurement. Since the information on the local blood flow has been obtained from the one-dimensional flow and Darcy models, the thermal effect of different vessels can be evaluated through the energy equation without other parameters.

Another characteristic of this study is that the image-based modeling method was employed to construct the finite element model. The realistic geometry of the finger can be constructed from medical images with a free image analysis program—Scion image [21] and our original code. Thus, the process is implemented with relative ease.

Further, the computational time can be significantly shortened as compared to that using a thorough two-dimensional model [25] to express the blood flow in living tissues.

One limitation of this method is that it requires the conversion of the one-dimensional blood velocity into the two-dimensional information in the finite element model. Additionally, the computation result of the blood temperature is easily affected by the mesh size, therefore, the mesh of the blood part should be created smaller than other parts.

In summary, the method based on the one-dimensional flow and the porous media transport model gives good results in analyzing heat transfer problems in living tissues. The proposed numerical method allows the processes from geometric modeling to hemodynamics and bioheat transfer analysis to be relatively easy to implement. Furthermore, through this computational advancement, 3D computational simulation in human extremities will be performed to effectively predict blood flow and thermoregulation behavior. Finally, the proposed method will allow the exploration of practical applications to personal health care and clinical therapies for understanding the physiological parameters through human fingers.

Conflict of interest statement

None declared.

References

[1] O.K. Cho, Y.O. Kim, H. Mitsumaki, K. Kuwa, Noninvasive measurement of glucose by metabolic heat conformation method, Clin. Chem. 50 (2004) 1894–1898.
[2] H.H. Pennes, Analysis of tissue and arterial blood temperatures in the resting human forearm, J. Appl. Physiol. 1 (2) (1948) 93–122.
[3] K.H. Keller, L. Seiler, An analysis of peripheral heat transfer in man, J. Appl. Physiol. 30 (5) (1971) 779–786.
[4] E.H. Wissler, A mathematical model of the human thermal system, Bull. Math. Biophy. 26 (1964) 147–166.
[5] C.K. Charny, R.L. Levin, A three-dimensional thermal and electromagnetic model of whole limb heating with a MAPA, IEEE Trans. Biomed. Eng. 38 (10) (1991) 1030–1037.
[6] T. Takemori, T. Nakajima, Y. Shoji, A fundamental model of the human thermal system for prediction of thermal comfort, Trans. JSME (B) 61 (584) (1995) 297–304.
[7] A. Shitzer, L. Stroschein, A.P. Vital, R.R. Gonzalez, K.B. Pandolf, Numerical analysis of an extremity in a cold environment including countercurrent arterio-venous heat exchange, Trans. ASME J. Biomech. Eng. 119 (1997) 179–186.
[8] Y. He, H. Liu, R. Himeno, M. Shirazaki, Numerical and experimental study on the relationship between blood circulation and peripheral temperature, J. Mech. Med. Biol. 5 (1) (2005) 39–53.
[9] M.M. Chen, K.R. Homles, Microvascular contributions in tissue heat transfer, Ann. N.Y. Acad. Sci. 335 (1980) 137–150.
[10] S. Weinbaum, L.M. Jiji, A new simplified bioheat equation for the effect of blood flow on local average tissue temperature, J. Biomech. Eng. 107 (1985) 131–139.
[11] H. Brinck, J. Werner, Estimation of the thermal effect of blood flow in a branching countercurrent network using a three-dimensional vascular model, Trans. ASME J. Biomech. Eng. 164 (1994) 324–330.

[12] A.R.A. Khaled, K. Vafai, The role of porous media in modeling flow and heat transfer in biological tissues, Int. J. Heat Mass Transfer 46 (2003) 4989–5003.
[13] W. Wulff, The energy conservation equation for living tissue, IEEE Trans. Biomed. Eng. 1974, 494–495.
[14] Y.M. Xuan, W. Roetzel, Bioequation of the human thermal system, Chem. Eng. Technol. 20 (1997) 269–276.
[15] Image-based biomechanics, Trans. JSME (A) 70(697) (2004) (special issue) (Japanese).
[16] J.R. Cebral, R. Löhner, From medical images to anatomically accurate finite element grids, Int. J. Numer. Meth. Eng. 51 (2001) 985–1008.
[17] C. Sheng, S.N. Sarwal, K.C. Watts, A.E. Marble, Computational simulation of blood flow in human systemic circulation incorporating an external force field, Med. Biol. Eng. Comput. 33 (1995) 8–17.
[18] M.S. Olufsen, C.S. Peskin, W.Y. Kim, E.R. Pedersen, A. Nadim, J. Larsen, Numerical simulation and experimental validation of blood flow in arteries with structured-tree outflow conditions, Ann. Biomed. Eng. 28 (2000) 1281–1299.
[19] M. Zagzoule, J. Marc-Vergnes, A global mathematical model of the cerebral circulation in man, J. Biomech. 19 (12) (1986) 1015–1022.
[20] Y. He, H. Liu, R. Himeno, A one-dimensional thermo-fluid model of blood circulation in the human upper limb, Int. Heat Mass Transfer 47 (2004) 2735–2745.
[21] ⟨http://www.scioncorp.com/⟩.
[22] H.S. Kou, T.C. Shih, W.L. Lin, Effect of the directional blood flow on thermal dose distribution during thermal therapy: an application of a Green's function based on the porous model, Phys. Med. Biol. 48 (2003) 1577–1589.
[23] D.A. Nield, A. Bejan, Convection in Porous Media, second ed., Springer, Berlin, 1998.
[24] K. Hirasawa, Anatomy: Angiology. Neurology, 1982, vol. 2, Kanehara Co. Ltd., p. 66 (in Japanese).
[25] Y. He, M. Shirazaki, R. Himeno, A finite element model for determining the effects of blood flow on the finger temperature distribution, in: Proceedings of the Sixth ASME-JSME Thermal Joint Conference, Hawaii, TED-AJ03-166, 2003.

Y. He received her B.E. (1989) and M.E. (1992) degrees from Dalian University of Technology, China, and the D.E. degree (1999) from The University of Tokyo, Japan. She works as a professor of Department of Modern Mechanics, University of Science and Technology of China. Her research interests include numerical and experimental studies of blood flow and heat transfer in living tissues.

H. Liu received his B.S. degree (1985) from Dalian University of Technology, China, and completed his M.S.E. (1989) and Ph.D. (1992) from Yokohama National University, Japan. He is a professor of the Department of Electronics and Mechanical Engineering in Chiba University. His research interests focus on computational fluid dynamics, biological fluid dynamics, physiological fluid dynamics, and image-based modeling of cardiovascular arterial vessels.

R. Himeno received his B.E. (1977) and M.E. (1979) degrees from Kyoto University and received the D.E. degree (1989) from The University of Tokyo. He is the unit leader of the Computational Biomechanics Unit and the director of the Advanced Center for Computing and Communication, RIKEN. His current interests include computational biomechanics simulation and structure-fluid coupled simulation.

J. Sunaga received her B.A. (2003) and M.A. (2005) degrees from Nihon University, Japan. She works as a contract researcher at the Computational Cell Biomechanics team of V-CAD system program RIKEN. Her interest is experimental analysis on the internal structure of biological sample.

N. Kakusho received his B.A. (1995) and M.A. (1997) degrees from Nihon University, Japan. He works as a contract researcher at the Computational Biomechanics Unit, RIKEN. He is interested in analyzing the internal structure of biological sample.

H. Yokota received his B.A. (1991) and M.A. (1993) degrees from Nihon University and received the D.E. degree (1999) from The University of Tokyo. He is the team leader of the Bio-research Infrastructure Construction Team and the contract researcher of the Computational Biomechanics Unit, RIKEN. His current interests include computational biomechanics simulation and structure modeling for industrial product and biological sample.